KJO
pISSN: 1011-8942 eISSN: 2092-9382

Korean J Ophthalmol 2012;26(5):347-354
http://dx.doi.org/10.3341/kjo.2012.26.5.347

Original Article

Morphologic Changes in Acute Central Serous Chorioretinopathy Using Spectral Domain Optical Coherence Tomography

Hyung Chan Kim, Won Bin Cho, Hyewon Chung

Department of Ophthalmology, Konkuk University Medical Center, Konkuk University School of Medicine, Seoul, Korea

Purpose: To investigate morphologic changes of acute central serous chorioretinopathy (CSC) using spectral domain optical coherence tomography (SD-OCT) and confocal scanning laser ophthalmoscopy.

Methods: This retrospective study included 63 eyes of 63 patients with unilateral acute CSC. All patients underwent simultaneous SD-OCT and fluorescein angiography examination using Spectralis HRA+OCT.

Results: The external limiting membrane could be seen on SD-OCT, although the junction between photoreceptor inner and outer segments (IS/OS) was not detected in all eyes with retinal detachment (RD). However, IS/OS became visible after resolution of serous RD in 51 eyes (81.0%). SD-OCT images at the leakage sites showed a bump of retinal pigment epithelium (RPE) in in 47 cases (68.1%) and pigment epithelial detachment (PED) in 22 of 69 leakage sites (31.9%). In 14 of 69 leakage sites (20.3%), highly reflective areas suggesting fibrinous exudate were observed in the subretinal space. In nine leakage sites (13.0%), sagging or dipping of the posterior retinal layer was seen. Abnormal RPE changes such as RPE bump and PED were observed in 12 of 22 fellow eyes (54.5%).

Conclusions: A variety of morphologic changes could be identified on SD-OCT, and those findings may contribute more information to our understanding of the pathophysiology of CSC.

Key Words: Central serous chorioretinopathy, Fluorescein angiography, Indocyanine green angiography, Leakage site, Spectral domain optical coherence tomography

Central serous chorioretinopathy (CSC) is characterized by idiopathic detachment of the neurosensory retina in the macular area, secondary to one or more retinal pigment epithelium (RPE) leakage points on fluorescein angiography (FA). The ocular manifestations in CSC have been thought to arise primarily from an abnormality of the RPE [1].

With indocyanine green angiography (ICGA), multifocal areas of choroidal vascular hyperpermeability in patients with CSC have been reported [2]. It has been shown that the leakage area at the level of RPE on FA was contiguous with the areas of choroidal vascular hyperpermeability on ICGA [2]. Some areas of choroidal hyperpermeability on ICGA were not associated with active fluorescein leaks on FA. Focal areas of ICGA hyperfluorescence were also noted in clinically asymptomatic fellow eyes [3]. Therefore, exudative changes within the choroid are considered to be the primary event in the disease, and the subsequent changes at the RPE allow the fluid to enter the subretinal space, resulting in neurosensory retinal detachment (RD). These hypotheses are based on FA and ICGA findings; however, the precise morphologic correlations have not yet been elucidated.

Optical coherence tomography (OCT) is a noninvasive technique for the cross-sectional imaging of the retina. Previous reports using OCT showed various features of CSC, including neurosensory RD, pigment epithelial detachment (PED), fibrinous exudates, and cystic changes within the retina. Recently, spectral domain OCT (SD-OCT) was introduced for advanced imaging that reduces acquisition time and allows for high resolution imaging of

Received: May 4, 2011 *Accepted*: November 17, 2011

Corresponding Author: Hyung Chan Kim, MD, PhD. Department of Ophthalmology, Konkuk University Medical Center, Konkuk University School of Medicine, #120 Neungdong-ro, Gwangjin-gu, Seoul 143-729, Korea. Tel: 82-10-7138-5657, Fax: 82-2-2030-5273, E-mail: eyekim@kuh.ac.kr

macular microstructures [4-9]. SD-OCT allows for the improved visualization of retinal structures, especially photoreceptor cell layers. Using Spectralis HRA+OCT (Heidelberg Engineering, Heidelberg, Germany), a combination of OCT and confocal scanning laser ophthalmoscopy (cSLO) in one instrument offers a number of subsequent advantages, including an exact correlation of the topographic architecture of the retina, which offers new insights into the pathogenesis and morphological alterations of various retinal diseases [10].

We investigated the microstructural changes of the retina, RPE, and leakage sites detected on FA in acute unilateral CSC using Spectralis HRA+OCT. We also studied their changes after resolution of subretinal fluid (SRF) with or without treatment.

Materials and Methods

We retrospectively investigated 63 eyes of 63 patients (47 men and 16 women) with first episode unilateral acute CSC from October 2008 to September 2009 at Konkuk University Medical Center. The average age of the patients was 44.7 ± 8.4 years (Table 1). All patients had undergone a complete ophthalmic examination, including measurement of best-corrected visual acuity (BCVA) using the Snellen visual acuity chart converted to logarithm of the minimum angle of resolution (logMAR) visual acuity, slit-lamp biomicroscopy with a noncontact fundus lens (SuperField lens; Volk Optical Inc., Mentor, OH, USA), and fundus photography with Topcon IMAGEnet Digital System and SD-OCT examination. SD-OCT imaging was performed with the Spectralis HRA+OCT according to the manufacturer's guidelines using linear and volume scanning. Retinal thickness was defined as the distance between the internal limiting membrane and Bruch's membrane using the computer-based caliper measurement tool in the Spectralis HRA+OCT system, and foveal thickness (FT) was calculated automatically. A dome-shaped protrusion of RPE with sub-RPE fluid was defined as a PED, and a small irregular protrusion of RPE without sub-RPE fluid was defined as an RPE bump. FA was also performed in all patients using Spectralis HRA+OCT. ICGA was performed on 44 eyes of 22 patients using the Topcon IMAGEnet Digital System for better visualization of choroidal vascular hyperpermeability in the mid or late phase.

Patients were observed without intervention for two to three months. After this period, focal laser photocoagulation in eyes with extrafoveal leakages or half-dose photodynamic therapy (PDT) in eyes with juxtafoveal or diffuse leakages was performed for patients for whom the SRF was not absorbed. Argon laser photocoagulation (spot size, 150-200 μm; duration, 0.1-0.2 second; power, 100-150 mW; number of shots, 1-2) was performed at leakage sites outside the perifoveal capillary network. The half-dose PDT protocol for CSC was performed using half the normal dose of verteporfin (Visudyne; Novartis AG, Bulach, Switzerland), 3 mg/m^2. Verteporfin was infused over eight minutes, followed by delivery of laser energy at 689 nm for 10 minutes from the commencement of infusion to target the area of choroidal dilation and hyperpermeability. A total light energy of 50 J/cm^2 was delivered over 83 seconds. Informed consent was obtained from all patients who underwent laser photocoagulation or PDT treatment. At 4 to 12 weeks after treatment, follow-up was continued with Spectralis HRA+OCT imaging with unique referencing technology which allows for imaging at the exact same point of the previous leakage site.

Table 1. Characteristics of the affected eyes and the fellow eyes

Variable	Value	
No. of eyes	63	
Age (yr)	44.7 ± 8.4	
Sex (men / women)	47 / 16	
Follow-up period (mon)	4.7 ± 2.1	
Baseline examination		
BCVA (logMAR)	0.21 ± 0.25	
Foveal thickness (μm)	528.8 ± 154.6	
Final examination after resolution		
BCVA (logMAR)	0.04 ± 0.07	($p < 0.001$)*
Foveal thickness (μm)	233.9 ± 27.3	($p < 0.001$)*
Fellow eyes		
BCVA (logMAR)	0.01 ± 0.03	($p < 0.001$)†
Foveal thickness (μm)	256.9 ± 23.4	($p = 0.028$)†

BCVA = best-corrected visual acuity; logMAR = logarithm of the minimum angle of resolution.
*Difference between baseline exam and final exam in the affected eyes (paired *t*-test); †Difference between final exam in the affected eyes and the fellow eyes (Student's *t*-test).

Results

At baseline examination, mean BCVA (logMAR) was 0.21 ± 0.25, and mean FT was 528.8 ± 154.6 μm. During a mean follow-up of 4.7 months, 25 patients (39.7%) and eight patients (12.7%) underwent laser photocoagulation and half-dose PDT, respectively. The resolution of SRF was confirmed in 14 and four of those patients after treatment, respectively. At final examination, mean BCVA (logMAR) was 0.04 ± 0.07, and mean FT was 233.9 ± 27.3 μm, representing significant changes compared with those at baseline ($p < 0.001$). Mean BCVA and FT of the unaffected fellow eye were 0.01 ± 0.03 and 256.9 ± 23.4 μm, respectively. These values were significantly different from the mean BCVA ($p < 0.001$) and mean FT ($p = 0.028$) of the affected eyes at the final examination (Table 1).

All eyes with neurosensory RD showed slightly reflec-

tive lines in the outer nuclear layer, which was thought to be the external limiting membrane (ELM). However, the highly reflective line considered as the junction between the photoreceptor inner and outer segments (IS/OS) was not detected. The outer photoreceptor layer of detached neurosensory retina above the clear subretinal space was irregularly thickened and granulated (Fig. 1). The IS/OS was visible after the resolution of serous RD in 51 eyes (81.0%) and was not visible in 12 eyes (19.0%) (Fig. 2). The mean BCVA (logMAR) of 51 eyes with visible IS/OS was 0.03 ± 0.05, and that of 12 eyes with invisible IS/OS was 0.14 ± 0.09. There was a statistically significant difference between the mean BCVA (logMAR) of eyes with visible IS/OS and that of eyes with invisible IS/OS ($p = 0.03$, Student's *t*-test).

After the resolution of serous RD, most of the affected eyes showed thinner FT than fellow eyes (Fig. 3A). FT ratio, calculated as FT of the affected eye divided by that of the fellow eye, showed a statistically significant correlation with BCVA ($r^2 = 0.614$, $p < 0.001$, Pearson's correlation coefficient) (Fig. 3B).

RPE abnormalities corresponding to the leakage sites were demonstrated in 63 of 69 eyes. SD-OCT images of the leakage sites showed PED in 22 (31.9%) (Fig. 4A) and a small bump of the RPE layers in 47 of 69 leakage sites (68.1%) (Fig. 4B). Overall, RPE abnormalities were found in all 69 leakage sites on SD-OCT (100%).

In 14 of 69 leakage sites (20.3%), a highly reflective area suggesting fibrinous exudate in the subretinal space was observed around the leakage site (Fig. 4B). In nine leakage sites (13.0%), sagging or dipping of the posterior layer of the neurosensory retina above the leakage site, which seemed to arise from the swelling of the outer nuclear layer due to the traction by fibrinous exudates, was observed (Fig. 4B). A minute defect in the RPE layer within the PED was observed in one leakage site (1.4%), and that defect corresponded exactly to a leakage site (Fig. 5).

ICGA was performed in 22 eyes, and choroidal vascular hyperpermeability was observed in all the affected eyes and 16 asymptomatic fellow eyes (72.7%). Furthermore, 12 fellow eyes (54.5%) showed abnormal RPE changes such as an RPE bump (Fig. 6A) and PED (Fig. 6B) on SD-OCT. SD-OCT findings of all the affected and fellow eyes in acute CSC are summarized in Fig. 7.

Follow-up SD-OCT was available in 17 of 25 eyes with focal laser treatment, 8 of 8 eyes with half-dose PDT, and ten eyes that did not receive treatment. The percentage of complete resolution of SRF in eyes without treatment was 70.0% (7 of 10 eyes), which was higher than that in eyes with half-dose PDT (50.0%, 4 of 8 eyes). However, focal laser or half-dose PDT was performed in only those patients whose SRF did not change after two to three months of observation. Both focal laser and half-dose PDT were effective for the resolution of SRF and resulted in improved vision. Pre- and post-treatment characteristics of the eyes are summarized in Table 2.

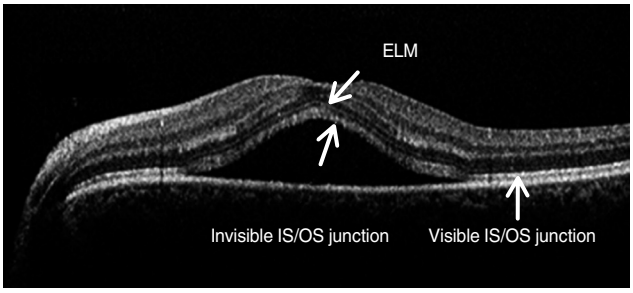

Fig. 1. Optical coherence tomography image of a 55-year-old woman with central serous chorioretinopathy. External limiting membrane (ELM) is clearly visible; however, the junction between photoreceptor inner and outer segments (IS/OS) is not detected in the detached neurosensory retina. The outer photoreceptor layer of the detached neurosensory retina above the clear subretinal space was irregularly thickened and granulated.

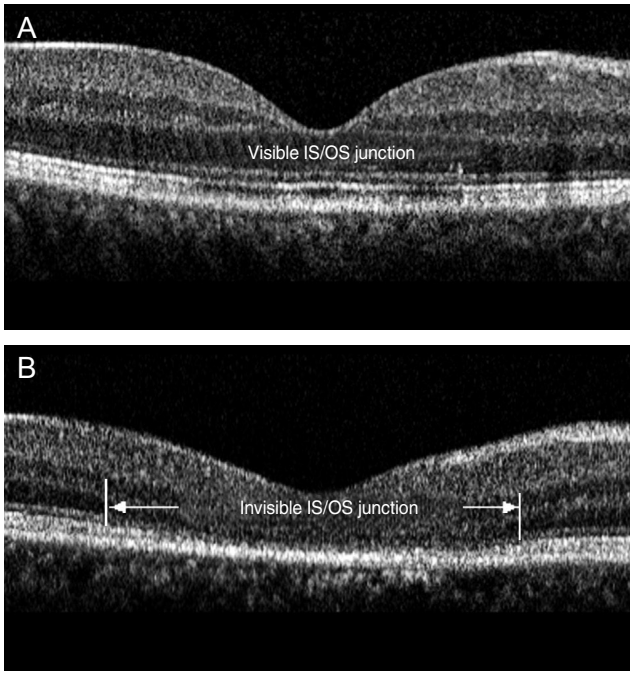

Fig. 2. Optical coherence tomography images of a 39-year-old man (A) and 46-year-old man (B) after resolution of serous detachment. (A) The junction of photoreceptor inner and outer segments (IS/OS) is intact and clearly visible. (B) IS/OS is disrupted and invisible.

Although IS/OS disruption was found at the extrafoveal area in eyes with focal laser treatment (9 of 17 eyes, 52.9%), no IS/OS disruption was detected at the fovea in eyes with focal laser treatment or half-dose PDT.

Discussion

Although the exact pathophysiology of CSC is not yet

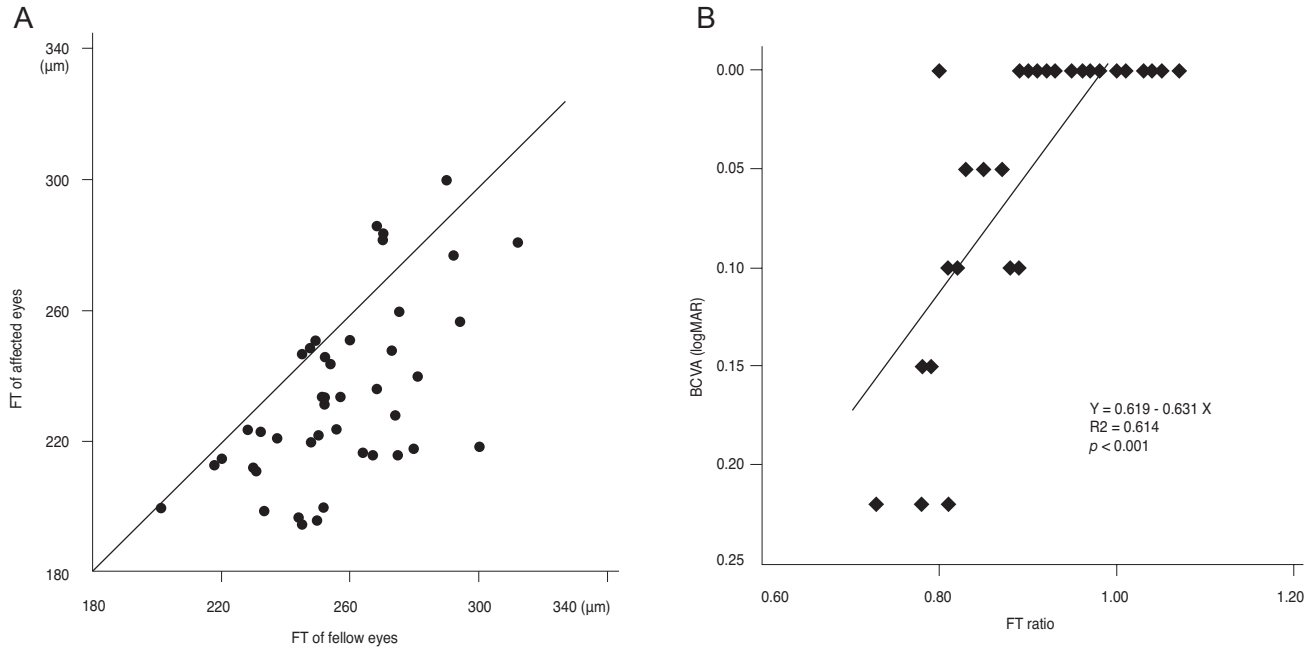

Fig. 3. (A) Distribution of foveal thickness (FT) of the affected eyes and the fellow eyes after resolution of serous detachment shows that most of the affected eyes have thinner FT than the fellow eyes. (B) FT ratio, the FT of the affected eye divided by that of the fellow eye, shows a significant positive correlation with best-corrected visual acuity (BCVA, logarithm of the minimum angle of resolution [logMAR]).

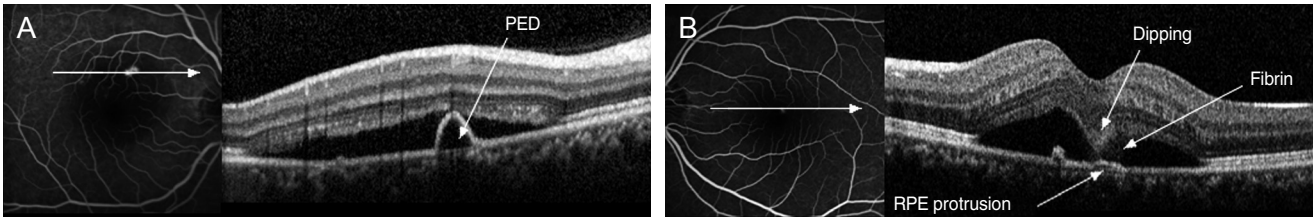

Fig. 4. Simultaneous imaging of fluorescein angiography and spectral domain optical coherence tomography (SD-OCT) in a 41-year-old man (A) and a 39-year-old man (B) with acute central serous chorioretinopathy. The horizontal linear scans of the SD-OCT image corresponding to the leakage sites show (A) pigment epithelial detachments (PED) and (B) retinal dipping above the retinal pigment epithelium (RPE) protrusion with fibrinous exudates in the subretinal space.

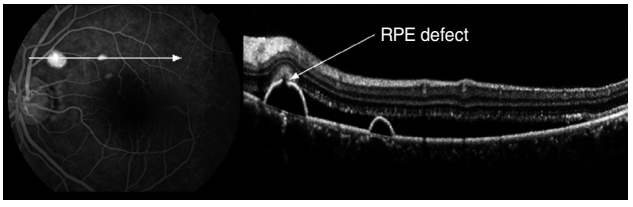

Fig. 5. Simultaneous imaging of fluorescein angiography (FA) and spectral domain optical coherence tomography (SD-OCT) in a 59-year-old woman with acute central serous chorioretinopathy. The minute defect in the retinal pigment epithelium (RPE) layer within the pigment epithelial detachment on SD-OCT corresponds exactly to a leakage point on FA.

fully understood, the primary pathology is thought to begin with disruption of the choroidal circulation. The RPE is then decompensated and allows exudate from the choroidal vasculature to pass into the subretinal space [2,11-14]. These hypotheses are based on FA and ICGA findings, and the precise morphologic changes and their correlations with FA or ICGA have not been clearly elucidated.

The various morphologic changes such as PED, subretinal fibrinous exudates, and retinal cystic changes in eyes with CSC were reported using conventional time domain OCT (TD-OCT) [15-18]. However, previous studies could not define the subtle changes of the retina because of the insufficient resolution of TD-OCT to distinguish the retinal layers.

With the advent of SD-OCT, the subtle changes of the outer retinal layers including ELM, photoreceptor layer, and RPE could be well defined. Recently, secondary changes of the outer retina in eyes with CSC using SD-OCT have been reported (Table 3).

In this study, we identified the microstructural morphol-

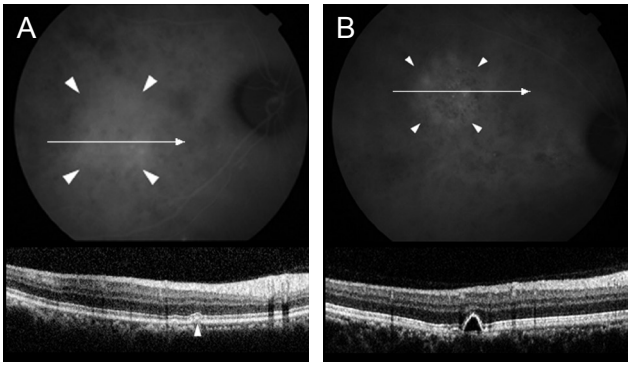

Fig. 6. Simultaneous imaging of indocyanine green angiography (ICGA) and spectral domain optical coherence tomography in asymptomatic fellow eyes. An retinal pigment epithelium bump (A) and pigment epithelial detachment (B) are observed at the area of choroidal vascular hyperpermeability on ICGA.

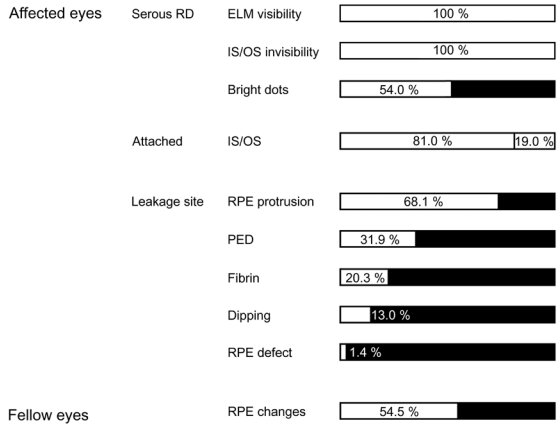

Fig. 7. The spectral domain optical coherence tomographic findings of all the affected and fellow eyes in our study. RD = retinal detachment; ELM = external limiting membrane; IS/OS = inner and outer segments; RPE = retinal pigment epithelium; PED = pigment epithelial detachment.

ogy of the detached retina using SD-OCT. The ELM was clearly visible in the detached retina on SD-OCT; however, the IS/OS was not detected in all eyes, similar to previous reports (Table 2). Ojima et al. [7] suggested that CSC primarily alters the photoreceptor outer segment (OS), and Fujimoto et al. [19] reported that the thickness of photoreceptor OS increased and the photoreceptor OS was changed to a granular appearance after several months in the acute phase, after which the thickness then gradually decreased. The granular appearance of the OS is thought to develop through accumulation of the shed OS. After retinal reattachment, the IS/OS gradually becomes clear, which implies normalization of the assembly of the photoreceptor OS by restored phagocytosis of shed discs of the photoreceptors by the RPE [20]. In our study, we identified these same morphologic changes on SD-OCT during the follow-up period.

The majority of patients with acute CSC have spontaneous resolution of serous RD and have a good visual prognosis. However, prolonged macular detachment may cause degenerative manifestations in the neurosensory retina, especially photoreceptor OS, resulting in a poor visual outcome [20-22]. We performed laser photocoagulation or half-dose PDT in patients with no changes in SRF during 2 to 3 months of observation.

The percentage of complete resolution of SRF in the observation group (70.0%, 7 of 10 eyes) was higher than that in the half-dose PDT group (50.0%, 4 of 8 eyes) and comparable to that in the focal laser group (82.4%, 14 of 17 eyes). However, either focal laser or half-dose PDT was applied to patients in whom SRF was not absorbed after the 2 to 3 month observation period. Thus, the percentage of complete resolution of SRF in the observation group was 20.0% (7 of 35 eyes), which was the lowest among the three groups (Table 2). Complete resolution of SRF was achieved most frequently by focal laser photocoagulation (82.4%). The treatment group, the focal laser group plus the half-dose PDT group, had better results regarding complete resolution of SRF than the observation group (18 of 25 eyes, 72% vs. 7 of 35 eyes, 20%; $p < 0.001$; chi-square test).

The complete resolution of SRF in the observation group occurred in only 20.0% of patients (7 of 35 eyes), although acute CSC is known to resolve spontaneously in about 80% of patients. The low rate of spontaneous resolution in our study could be explained by the loss of patients to follow-up. This study included 63 eyes of 63 patients with acute CSC at baseline. However, 28 patients did not return to the clinic after their first visits, and it was assumed that spontaneous resolution of SRF led to the improvement of symptoms in those patients. If all of those 28 patients are considered to have had spontaneous resolution, the percentage of spontaneous resolution in this study would then be 55.6% (35 of 63 eyes), which is much higher than the 20% in the observation group.

In addition, no IS/OS disruption in the fovea in eyes with half-dose PDT or laser photocoagulation treatment was found. These results suggest that half-dose PDT might be a safe and effective option for eyes with subfoveal or juxtafoveal leakage on FA and hyperpermeability on ICGA. Most of the affected eyes had thinner FT than fellow eyes after the resolution of serous RD in this study, and BCVA at the final visit was higher in patients with a high FT ratio. This finding suggests that photoreceptors can be damaged to some degree during the serous RD in CSC, although other retinal layers might also be affected. Matsumoto et al. [23] showed that the outer nuclear layer thickness measured by SD-OCT is positively correlated with the BCVA in resolved CSC.

Previous studies using TD-OCT have reported on the

Table 2. Pre- and post-treatment characteristics

	No. of eyes	Follow-up period (day)	Pre-treatment				Post-treatment		
			RPE lesion at leakage		BCVA (logMAR ± SD)	FT (μm ± SD)	Complete resolution of SRF	BCVA (logMAR ± SD)	FT (μm ± SD)
			Irregular RPE	PED					
Focal laser	17	41.6 ± 14.2	13	4	0.24 ± 0.20	479.4 ± 130.3	14 / 17 (82.4%)	0.09 ± 0.14	257.9 ± 51.8
Half-dose PDT	8	31.5 ± 2.7	6	2	0.24 ± 0.19	478.0 ± 93.00	4 / 8 (50.0%)	0.08 ± 0.10	241.3 ± 34.5
Observation	10	59.0 ± 20.2*	9	1	0.24 ± 0.31	511.1 ± 142.9	7 / 35 (20.0%)†	0.05 ± 0.06	290.8 ± 83.5
p-value		0.005‡	0.643§		0.824‡	0.603‡	<0.001§	0.850‡	0.299‡

RPE = retinal pigment epithelium; PED = pigment epithelial detachment; BCVA = best-corrected visual acuity; logMAR = logarithm of the minimum angle of resolution; SD = standard deviation; FT = foveal thickness; SRF = subretinal fluid; PDT = photodynamic therapy.
*Duration from the onset of the symptom to complete resolution of SRF or final follow-up; †A total of 35 patients include 25 treated patients whose SRF was not spontaneously resolved despite 2 to 3 months of observation; ‡Kruskal-Wallis test; §Chi-square test.

Table 3. Reported frequency (%) of spectral domain optical coherence tomography findings in acute central serous chorioretinopathy

	Detached retina							Resolved retina	Fellow eye
	Visible ELM	Invisible IS/OS	Leakage site					Visible IS/OS	RPE changes
			RPE bump	PED	Fibrin	Dipping	RPE defect		
Mitarai et al. 2006			33*	63					
Ojima et al. 2007	95	100						100 (4/4)	
Matsumoto et al. 2008	100	100							
Fujimoto et al. 2008			35	61	52	43	13		
Shinojima et al. 2010			29	71	62		10		
Our study	100	100	68	32	20	13	1	81	55

ELM = external limiting membrane; IS/OS = inner and outer segment; RPE = retinal pigment epithelium; PED = pigment epithelial detachment.
*Rough RPE + PED bump.

morphologic changes of RPE [15-17,24]. However, it was difficult to confirm that such RPE changes corresponded precisely to the leakage sites on FA. One of the spectacular properties of the Spectralis HRA+OCT is the multiple imaging modalities with an eye tracking system. It has the ability to perform FA or ICGA simultaneously with SD-OCT. Therefore, the simultaneous imaging of FA or ICGA with SD-OCT allows us to identify the configurations of morphologic RPE changes at the leakage sites in eyes with CSC. Using Spectralis HRA+OCT, RPE abnormalities corresponding to leakage sites were precisely demonstrated in 69 leakage sites of 63 eyes. SD-OCT images of the leakage sites showed PED in 22 eyes (31.9%) (Fig. 4A) and a small bump of the RPE layer in 47 of 69 leakage sites (68.1%) (Fig. 4B). In previous reports, PED was found in 61% to 71% of leakage sites (Table 2). We considered small or atypical PEDs as RPE abnormalities, explaining why PED was much lower in our study compared with previous studies. On the other hand, Shinojima et al. [25] reported a high incidence of PED (71%) also using the Spectralis HRA+OCT. They suggested that SD-OCT allowed the detection of small or shallow PEDs, which was not previously possible. In addition, SD-OCT and cSLO enabled us to detect these very small PEDs by examining the area in proximity of the leakage point. Although incidences of PED differed between the study by Shinojima et al. and the present study, both studies observed RPE abnormalities (RPE irregularity or PED) in all of the involved eyes.

Montero and Ruiz-Moreno [24] reported that similar RPE changes, which they described as small RPE bulges, could be observed with TD-OCT, and they suggested that those lesions were related to angiographic leakage sites in 35 of 36 eyes with CSC. We identified the same findings in detail with high precision using the simultaneous imaging technology of Spectralis HRA+OCT. We speculate that those changes might indicate a minimal PED or PED with subpigment epithelial exudates. It is believed that a focal increase in permeability of the choriocapillaris might be the primary cause of damage to the overlying RPE in patients with CSC [2]. Therefore, hydrostatic pressure caused by hyperpermeability may cause PED or an RPE bump. RPE abnormalities were found in all 69 leakage sites on SD-OCT (100%), suggesting that RPE abnormalities such as PED and RPE bumps at leakage sites are involved in the pathophysiology of CSC.

Perkins et al. [26] postulated that PEDs in CSC are a

sign of larger areas of compromised RPE. Focal leaks or defects of the RPE alone do not cause accumulation of SRF unless diffuse RPE dysfunction is present. In the current study, we observed a minute defect of the RPE within PED, which corresponded precisely to the leakage site on FA in one eye. The absence of RPE at the leakage site might be supported by the recent findings of fundus autofluorescence [27]. Eandi et al. [27] observed focal areas of hypoautofluorescence corresponding to the site of the focal RPE leak in acute CSC and suggested that the hypoautofluorescence may be blowout of the RPE at or near the junction of the attached and detached RPE. However, the hypoautofluorescence corresponding to the leakage site was not seen in all eyes with CSC, similar to the results in our study. We found focal areas of hypoautofluorescence corresponding precisely to the sites of the focal RPE leakage on FA in two eyes. A defect is usually too small to be detected even by SD-OCT or fundus autofluorescence analysis, although all eyes with acute CSC had a RPE defect at the leakage site.

Abnormal ICGA hyperfluorescence in clinically asymptomatic fellow eyes is well known [3]. In our study, we found an RPE bump in 12 eyes and PED in 16 asymptomatic fellow eyes with ICG hyperfluorescence. Furthermore, we were not able to find any RPE abnormalities in the areas without ICG hyperfluorescence. These findings support the choroidal origin theory of CSC that choroidal vascular hyperpermeability may cause the RPE defect, and that exudates escape to the subretinal space through this defect. The exact pathophysiology of RPE bumps in the asymptomatic fellow eyes of patients with CSC is not well defined. However, we speculate that a combination of choroidal vascular hyperpermeability and impaired RPE function leads to pooling of fluid in the subRPE space, which results in RPE bumps. These bumps might represent a preclinical or subclinical state of the disease. The exact pathophysiology of RPE bumps remains to be elucidated. The findings of this study corroborate the belief that CSC is essentially a bilateral asymmetric disease that causes morphologic alterations of the RPE in both eyes.

In conclusion, we identified a variety of microstructural changes using SD-OCT in CSC, and those findings contribute to our understating of the pathophysiology of CSC.

Conflict of Interest

No potential conflict of interest relevant to this article was reported.

References

1. Gass JD. Pathogenesis of disciform detachment of the neuroepithelium. *Am J Ophthalmol* 1967;63 Suppl:1-139.
2. Guyer DR, Yannuzzi LA, Slakter JS, et al. Digital indocyanine green videoangiography of central serous chorioretinopathy. *Arch Ophthalmol* 1994;112:1057-62.
3. Spaide RF, Campeas L, Haas A, et al. Central serous chorioretinopathy in younger and older adults. *Ophthalmology* 1996;103:2070-9.
4. Alam S, Zawadzki RJ, Choi S, et al. Clinical application of rapid serial fourier-domain optical coherence tomography for macular imaging. *Ophthalmology* 2006;113:1425-31.
5. Chen TC, Cense B, Pierce MC, et al. Spectral domain optical coherence tomography: ultra-high speed, ultra-high resolution ophthalmic imaging. *Arch Ophthalmol* 2005;123:1715-20.
6. Hangai M, Ojima Y, Gotoh N, et al. Three-dimensional imaging of macular holes with high-speed optical coherence tomography. *Ophthalmology* 2007;114:763-73.
7. Ojima Y, Hangai M, Sasahara M, et al. Three-dimensional imaging of the foveal photoreceptor layer in central serous chorioretinopathy using high-speed optical coherence tomography. *Ophthalmology* 2007;114:2197-207.
8. Wojtkowski M, Bajraszewski T, Gorczynska I, et al. Ophthalmic imaging by spectral optical coherence tomography. *Am J Ophthalmol* 2004;138:412-9.
9. Wojtkowski M, Srinivasan V, Fujimoto JG, et al. Three-dimensional retinal imaging with high-speed ultrahigh-resolution optical coherence tomography. *Ophthalmology* 2005;112:1734-46.
10. Wolf-Schnurrbusch UE, Enzmann V, Brinkmann CK, Wolf S. Morphologic changes in patients with geographic atrophy assessed with a novel spectral OCT-SLO combination. *Invest Ophthalmol Vis Sci* 2008;49:3095-9.
11. Iida T, Kishi S, Hagimura N, Shimizu K. Persistent and bilateral choroidal vascular abnormalities in central serous chorioretinopathy. *Retina* 1999;19:508-12.
12. Piccolino FC, Borgia L. Central serous chorioretinopathy and indocyanine green angiography. *Retina* 1994;14:231-42.
13. Prunte C, Flammer J. Choroidal capillary and venous congestion in central serous chorioretinopathy. *Am J Ophthalmol* 1996;121:26-34.
14. Scheider A, Nasemann JE, Lund OE. Fluorescein and indocyanine green angiographies of central serous choroidopathy by scanning laser ophthalmoscopy. *Am J Ophthalmol* 1993;115:50-6.
15. Hussain N, Baskar A, Ram LM, Das T. Optical coherence tomographic pattern of fluorescein angiographic leakage site in acute central serous chorioretinopathy. *Clin Experiment Ophthalmol* 2006;34:137-40.
16. Iida T, Hagimura N, Sato T, Kishi S. Evaluation of central serous chorioretinopathy with optical coherence tomography. *Am J Ophthalmol* 2000;129:16-20.
17. Kamppeter B, Jonas JB. Central serous chorioretinopathy imaged by optical coherence tomography. *Arch Ophthalmol* 2003;121:742-3.
18. Mitarai K, Gomi F, Tano Y. Three-dimensional optical coherence tomographic findings in central serous chorioretinopathy. *Graefes Arch Clin Exp Ophthalmol* 2006;244:1415-20.
19. Fujimoto H, Gomi F, Wakabayashi T, et al. Morphologic changes in acute central serous chorioretinopathy evaluated by fourier-domain optical coherence tomography. *Ophthalmology* 2008;115:1494-500, 1500.e1-2.
20. Matsumoto H, Kishi S, Otani T, Sato T. Elongation of photoreceptor outer segment in central serous chorioretinopathy. *Am J Ophthalmol* 2008;145:162-8.
21. Jalkh AE, Jabbour N, Avila MP, et al. Retinal pigment epi-

thelium decompensation. I. Clinical features and natural course. *Ophthalmology* 1984;91:1544-8.
22. Yannuzzi LA, Shakin JL, Fisher YL, Altomonte MA. Peripheral retinal detachments and retinal pigment epithelial atrophic tracts secondary to central serous pigment epitheliopathy. *Ophthalmology* 1984;91:1554-72.
23. Matsumoto H, Sato T, Kishi S. Outer nuclear layer thickness at the fovea determines visual outcomes in resolved central serous chorioretinopathy. *Am J Ophthalmol* 2009;148:105-10.e1.
24. Montero JA, Ruiz-Moreno JM. Optical coherence tomography characterisation of idiopathic central serous chorioretinopathy. *Br J Ophthalmol* 2005;89:562-4.
25. Shinojima A, Hirose T, Mori R, et al. Morphologic findings in acute central serous chorioretinopathy using spectral domain-optical coherence tomography with simultaneous angiography. *Retina* 2010;30:193-202.
26. Perkins SL, Kim JE, Pollack JS, Merrill PT. Clinical characteristics of central serous chorioretinopathy in women. *Ophthalmology* 2002;109:262-6.
27. Eandi CM, Ober M, Iranmanesh R, et al. Acute central serous chorioretinopathy and fundus autofluorescence. *Retina* 2005;25:989-93.